



RESEARCH PAPER

Effects of mavacamten on Ca²⁺ sensitivity of contraction as sarcomere length varied in human myocardium

Peter O. Awinda¹ | Yemeserach Bishaw¹ | Marissa Watanabe¹ | Maya A. Guglin³ |
Kenneth S. Campbell^{2,3}  | Bertrand C. W. Tanner¹ 

¹Department of Integrative Physiology and Neuroscience, Washington State University, Pullman, Washington, USA

²Department of Physiology, University of Kentucky, Lexington, Kentucky, USA

³Division of Cardiovascular Medicine, University of Kentucky, Lexington, Kentucky, USA

Correspondence

Bertrand C. W. Tanner, Department of Integrative Physiology and Neuroscience, Washington State University, Room 255 Vet/Biomed Research Building, 1815 Ferdinand's Lane, Pullman, WA 99164-7620, USA.
Email: bertrand.tanner@wsu.edu

Funding information

American Heart Association, Grant/Award Numbers: 17SDG33370153, 19TPA34860008, GRNT25460003; National Institutes of Health, Grant/Award Numbers: HL133358, HL144664, TR001988, R01HL149164; National Science Foundation, Grant/Award Number: 1656450

Background and Purpose: Heart failure can reflect impaired contractile function at the myofilament level. In healthy hearts, myofilaments become more sensitive to Ca²⁺ as cells are stretched. This represents a fundamental property of the myocardium that contributes to the Frank–Starling response, although the molecular mechanisms underlying the effect remain unclear. Mavacamten, which binds to myosin, is under investigation as a potential therapy for heart disease. We investigated how mavacamten affects the sarcomere-length dependence of Ca²⁺-sensitive isometric contraction to determine how mavacamten might modulate the Frank–Starling mechanism.

Experimental Approach: Multicellular preparations from the left ventricular-free wall of hearts from organ donors were chemically permeabilized and Ca²⁺ activated in the presence or absence of 0.5-μM mavacamten at 1.9 or 2.3-μm sarcomere length (37°C). Isometric force and frequency-dependent viscoelastic myocardial stiffness measurements were made.

Key Results: At both sarcomere lengths, mavacamten reduced maximal force and Ca²⁺ sensitivity of contraction. In the presence and absence of mavacamten, Ca²⁺ sensitivity of force increased as sarcomere length increased. This suggests that the length-dependent activation response was maintained in human myocardium, even though mavacamten reduced Ca²⁺ sensitivity. There were subtle effects of mavacamten reducing force values under relaxed conditions (pCa 8.0), as well as slowing myosin cross-bridge recruitment and speeding cross-bridge detachment under maximally activated conditions (pCa 4.5).

Conclusion and Implications: Mavacamten did not eliminate sarcomere length-dependent increases in the Ca²⁺ sensitivity of contraction in myocardial strips from organ donors at physiological temperature. Drugs that modulate myofilament function may be useful therapies for cardiomyopathies.

KEYWORDS

cardiac muscle mechanics, human myosin, mavacamten, sarcomere length

1 | INTRODUCTION

Cardiovascular disease remains a leading cause of death worldwide. Heart failure develops when the organ's ability to pump blood is compromised and elevated filling pressures are required to maintain adequate circulation (Borlaug & Paulus, 2011; Mozaffarian et al., 2016). Heart failure is a growing health problem affecting ~30 million people worldwide, with 50% of patients dying within 5 years of diagnosis (Ambrosy et al., 2014; Mozaffarian et al., 2016). The causes of heart failure are multifactorial, but dysregulated myofilament function within the sarcomere is a leading contributor. Recently, multiple pharmaceutical compounds have been developed to directly influence myofilament protein function as potential new therapies for heart disease (Cleland et al., 2011; Green et al., 2016; Grillo et al., 2018; Heitner et al., 2019; Kawas et al., 2017; Malik et al., 2011; Teerlink et al., 2016).

Cardiac muscle contraction is powered by cyclic interactions between myosin cross-bridges along thick filaments and actin-binding sites along thin filaments (Huxley & Hanson, 1954; Lymn & Taylor, 1971). Contractility is modulated by several well-known mechanisms including, (i) Ca^{2+} regulation via the thin-filament proteins troponin and tropomyosin, which modulates the number of available actin binding on a thin filament as intracellular $[\text{Ca}^{2+}]$ rises and falls throughout a heartbeat and (ii) thick-to-thin filament overlap, which determines how many cross-bridges are close enough to bind with Ca^{2+} -activated sites on actin. A mechanosensitive thick-filament regulatory mechanism has also been discovered, whereby myosin heads transition between OFF (also called the super-relaxed state or interacting heads motif) and ON states (also called the disordered-relaxed state) (Campbell, 2017; Hooijman et al., 2011). Heads in the OFF state are unable to bind actin (Figure 1), whereas those in the ON state can form cross-bridges by attaching to actin (Anderson et al., 2018; Liu et al., 2018; Rohde et al., 2018; Spudich, 2015). OFF-ON transitions can be very dynamic (Fusi et al., 2017; Piazzesiet al., 2018; Reconditi et al., 2017) and equilibrium kinetics are known to be regulated by (i) biochemical and steric interactions with thick-filament regulatory proteins (regulatory light chain; Kampourakis et al., 2016; Toepfer et al., 2013; Zhang et al., 2017; and cardiac myosin-binding protein-C; McNamara et al., 2017; McNamara et al., 2015) as well as (ii) myocardial force levels (Ait-Mou et al., 2016; Campbell et al., 2018; Fusi et al., 2016; Kampourakis et al., 2016; Linari et al., 2015). These multiple regulation pathways combine to influence length-dependent activation of contraction, wherein the myofilaments become more sensitive to Ca^{2+} as muscle cells are stretched. Length-dependent activation is an important cellular-level mechanism that underpins the Frank-Starling mechanism and enables the heart to increase cardiac output in response to elevated filling pressure.

The relative impact of thick- and thin-filament regulatory processes becomes difficult to separate, given myriad allosteric protein interactions along and between the filaments (reviewed by Gordon et al., 2000). These interactions facilitate the large change in force given a small change in $[\text{Ca}^{2+}]$, illustrated by the Hill

What is already known

- Mavacamten binds to myosin, slows myosin ATPase and stabilizes the myosin OFF state.
- Mavacamten is currently being tested in clinical trials for hypertrophic cardiomyopathy.

What this study adds

- Mavacamten reduces isometric force and Ca^{2+} sensitivity of contraction in human myocardial strips at body temperature.
- Length-dependent increases in Ca^{2+} sensitivity are maintained in presence of 0.5- μM mavacamten.

What is the clinical significance

- Drugs that modulate myofilament function are potential therapies for heart disease.
- The OFF-ON equilibrium of myosin may be a particularly important therapeutic target.

coefficients of the isometric force-pCa relationship being greater than 1. Dynamic changes in myocardial force influence regulatory coupling as well (Figure 1), where increased force during a cardiac twitch pulls additional myosin heads from OFF to ON (Brunello et al., 2020). As the thin filaments become Ca^{2+} activated, the ON heads will begin to actively generate force, which can further shift the pool of myosin heads from OFF to ON, thereby dynamically increasing cross-bridge binding and myocardial force production. It is also plausible that the opposite occurs during diastole to facilitate relaxation. Dynamic filament coupling enables robust activation and deactivation of contraction in health. Mechanisms that impair dynamic coupling can lead to dysfunctional contraction and relaxation with progression of heart disease (Campbell, 2017; Sparrow et al., 2019, 2020; Toepfer et al., 2016, 2020).

Mavacamten (formerly known as MYK-461; MyoKardia Inc.) is a drug under investigation to treat cardiac hypercontractility, a phenotype commonly associated with a form of heart disease called hypertrophic cardiomyopathy (Green et al., 2016; Stern et al., 2016; Toepfer et al., 2020). Hypertrophic cardiomyopathy affects 1:200 people and it is commonly associated with mutations in sarcomeric proteins. Although penetrance is highly variable, the mutations have been linked to elevated myocardial activation at low intracellular $[\text{Ca}^{2+}]$ during diastole (Semsarian et al., 2015; Van Der Velden et al., 2018). This can impair relaxation and precede

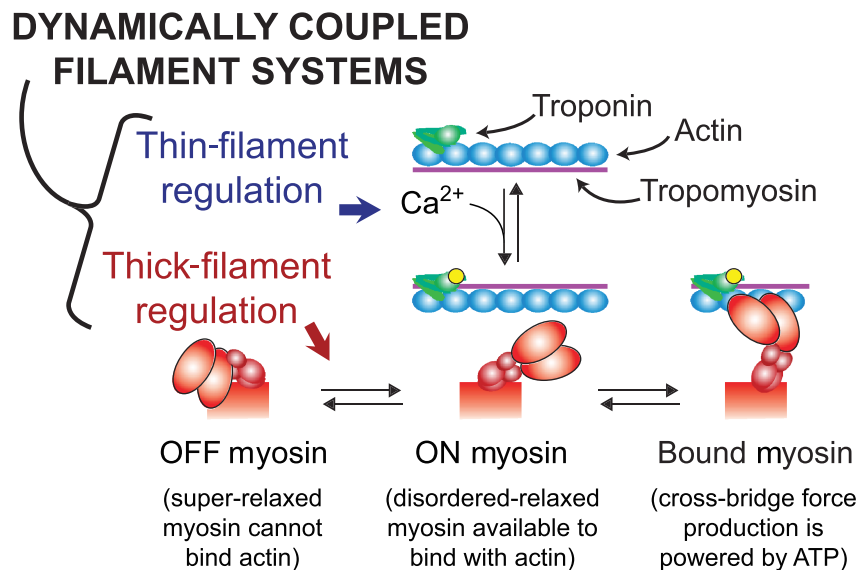


FIGURE 1 Schematic introducing dynamic filament coupling between thick and thin filaments. Thin-filament regulation involves Ca^{2+} binding to troponin and subsequent movement of tropomyosin to expose actin sites along the thin filament, to which myosin can bind and form force-generating cross-bridges. Thick-filament regulation involves myosin OFF–ON transition kinetics, which is a mechanosensitive equilibrium that shifts myosin heads from OFF to ON as muscle force increases. Myosin heads in the OFF state (also called the super-relaxed state) cannot bind actin, whereas those in the ON state (also called the disordered-relaxed state) can bind actin to form force-generating cross-bridges. This dynamic regulatory coupling implies that any modification to thin-filament function will in turn change the status of thick-filament regulation and vice versa (figure adapted from Campbell et al., 2018)

the development of hypertrophy. Contractile function during systole is often preserved or even enhanced (Ho et al., 2009; Michels et al., 2009). As the disease progresses, the ventricular walls thicken and stiffen, impairing ventricular filling and reducing cardiac output (Brandt et al., 1967; Klein et al., 1965; Maron et al., 1995; Semsarian et al., 2015; Stewart et al., 1968; Wilson et al., 1967).

Mavacamten binds to myosin, inhibits actin–myosin ATPase activity and stabilizes the myosin OFF state (Anderson et al., 2018; Green et al., 2016; Rohde et al., 2018; Toepfer et al., 2019, 2020). Solution biochemistry, *in vitro* motility and single molecule assays have shown that mavacamten slows the rates of inorganic phosphate (Pi) and ADP release (Green et al., 2016; Kawas et al., 2017; Rohde et al., 2018). Mavacamten also slows the rate of cross-bridge recruitment in skinned rodent myocardium (Mamidi et al., 2018), consistent with the idea of slowed myosin attachment and Pi release reducing cross-bridge force production. Increased concentrations of mavacamten reduced sarcomere shortening and accelerated relaxation in isolated electrically paced myocytes (Sparrow et al., 2019; Sparrow et al., 2020; Toepfer et al., 2019, 2020). Using genetically encoded calcium probes conjugated to troponin T and troponin I, Sparrow et al. (2019) showed that mavacamten reduced calcium activation at the myofilament, evident via reducing the time to 50% peak calcium binding, the time to 50% calcium release, and relative peak height of the calcium transient in electrically paced Guinea pig cardiomyocytes. These effects had not been apparent in prior studies using cytosolic calcium-sensing dyes (Green et al., 2016; Toepfer

et al., 2019, 2020). Although there are mixed findings with respect to mavacamten either reducing or not affecting Ca^{2+} sensitivity of contraction in skinned myocardial strips (Green et al., 2016; Mamidi et al., 2018), studies have shown that mavacamten consistently reduces maximal force production (Anderson et al., 2018; Green et al., 2016; Mamidi et al., 2018).

The effects of mavacamten on myosin force production and ATPase activity suggest that mavacamten may reduce hypercontractility and improve diastolic relaxation by depressing activity of the myosin motor (Heitner et al., 2019; Tuohy et al., 2020). However, the mechanisms through which mavacamten affects myosin cross-bridge kinetics and its potential effects on length-dependent myocardial function (i.e. the cellular basis of the Frank–Starling law) remain unclear. Therefore, we tested the effect of mavacamten on Ca^{2+} -activated force production at 1.9- and 2.3- μm sarcomere length in permeabilized myocardial strips from organ donors.

2 | METHODS

2.1 | Human tissue samples

Cardiac samples were obtained from six organ donors (two males and four females) at the University of Kentucky (Table 1). Their mean age was 45.5 (range 10–61) years. As previously described in detail (Blair et al., 2016), hearts were passed to a researcher as soon as they were

TABLE 1 Organ donor characteristics

Sample ID	Age (year)	Sex	Race	Diabetic	Cause of Death
FC3CB	10	F	White ^a	No	Anaphylaxis, anoxia
24713	47	F	White ^a	No	Head trauma
BE497	56	M	Black	No data	Cardiac arrest
31331	58	F	White ^a	No	Anoxia
CF462	61	F	White ^a	Yes	Stroke
2508D	41	M	White	No data	Stroke

^aNot Hispanic or Latino.

excised from the body, immediately placed in ice cold saline slush and transported back to the laboratory where tissue samples (~500 mg) were snap frozen in liquid nitrogen and stored at -150°C within ~20 min. Mid-myocardial sections of the left ventricular free wall were shipped overnight on dry ice to Washington State University and stored at -80°C for 1–3 weeks, until they were dissected for mechanics and biochemical experiments. All procedures were approved by the University of Kentucky Institutional Review Board.

2.2 | Materials

2.3 | Solutions

Muscle mechanics solution concentrations were formulated by solving equations describing ionic equilibria (Godt & Lindley, 1982) and all concentrations are listed in mM unless otherwise noted. All chemicals were purchased from Sigma (St. Louis, MO, USA) unless otherwise noted. Skinning solution is as follows: 50 BES, 30.83 K propionate, 10 Na azide (Fisher; Fair Lawn, NJ, USA), 20 EGTA, 6.29 MgCl_2 (J.T. Baker; Center Valley, PA, USA), 6.09 ATP, 1 DTT, 20 BDM (Acros Organics; Fair Lawn, NJ, USA), 50 Leupeptin (Peptides International; Louisville, KY, USA), 275 Pefabloc (Acros Organics) and 1 E-64 (Peptides International); with 1% Triton-X100 (wt/vol) and 50% glycerol (wt/vol; J.T. Baker). Storage solution is the same as skinning solution without Triton-X100. Relaxing solution is as follows: pCa 8.0 (pCa = $-\log_{10}[\text{Ca}^{2+}]$), 5 EGTA, 5 MgATP, 1 Mg^{2+} , 0.3 P_i , 35 phosphocreatine, 300 U/ml of creatine kinase, pH 7.0, at 200 ionic strength adjusted with Na methanesulfonate. Activating solution is as follows: same as relaxing solution but with pCa 4.5.

Mavacamten (MYK-461) was purchased from Axon Medichem (Reston, VA, USA) and dissolved in DMSO (J.T. Baker) to give a 1-mM stock solution. This was then mixed with relaxing and activating solutions to yield experimental solutions containing 0.5- μM mavacamten and 0.05% DMSO (vol/vol). The 0.5- μM mavacamten concentration was chosen as an intermediate between the IC_{50} value of 0.3 μM for inhibiting myosin ATPase activity in biochemical assays using murine and bovine myosin (Green et al., 2016) and plasma levels that effectively relieved left ventricular outflow tract obstruction in clinical trial patients (350–695 ng/ml = 1.28–2.54 μM ; Heitner et al., 2019).

2.4 | Mechanical measurements using permeabilized myocardial strips

Frozen tissue sections were thawed in ice-cold skinning solution and dissected into thin strips (~180 μm in diameter and 700 μm long). These were skinned overnight at 4°C , transferred to storage solution and stored at -20°C for 0–5 days. On the day of experiments, strips were mounted between a motor (P841.40, Physik Instrumente, Auburn, MA) and a strain gauge (AE801, Kronex, Walnut Creek, CA), lowered into a 30- μl droplet of relaxing solution (with or without mavacamten) and stretched to a sarcomere length of 1.9 or 2.3 μm as measured by digital Fourier transform analysis (IonOptix Corp, Milton, MA). Mounting and measurement of strip dimensions take roughly 10–15 min prior to making any tension measurements, thereby reflecting the duration that a strip would have been exposed to mavacamten prior to any mechanics measurements. The maximal effect of mavacamten on cellular contractility occurred within a 5-min incubation time and longer incubations (up to an hour) did not produce any detrimental effects on contractility (Sparrow et al., 2020). Solutions were maintained at body temperature (37°C) throughout each experiment, using 2–3 strips at each condition for each heart. The type of experiment for each myocardial strip (i.e. treatment group and sarcomere length) was randomized.

Strips were activated in solutions (with or without mavacamten) at pCa values ranging from 8.0 to 4.5 to measure the steady-state, isometric force–pCa relationship. Force values were normalized to the cross-sectional area of each preparation and reported as stress values with units of $\text{kN}\cdot\text{m}^{-2}$. Stress–pCa curves from each strip were fit to a 4-parameter Hill equation using MATLAB (version 9.0.4, Mathworks, Natick, MA, RRID:SCR_001622)

$$\text{Stress (pCa)} = F_{\text{pas}} + \frac{F_{\text{act}}}{1 + 10^{n_H(\text{pCa} - \text{pCa}_{50})}}, \quad (1)$$

where F_{pas} corresponds to passive stress under relaxed conditions, F_{act} corresponds to maximal Ca^{2+} -activated stress, pCa_{50} represents the free Ca^{2+} concentration required to develop half the maximum Ca^{2+} -activated stress and n_H is the Hill coefficient.

Sinusoidal length perturbations of 0.125% myocardial strip length (clip-to-clip) were applied at 41 discrete frequencies from 0.125 to 100 Hz to measure the complex modulus as a function of angular

frequency (Kawai & Brandt, 1980; Mulieri et al., 2002; Palmer et al., 2007). The complex modulus represents viscoelastic myocardial stiffness, which arises from the change in stress divided by the change in muscle length that is in-phase (elastic modulus) and out-of-phase (viscous modulus) with the oscillatory length change at each frequency.

Characteristics of the elastic and viscous moduli responses over the measured frequency range provide a signature of cross-bridge binding and cycling kinetics. Shifts in the elastic modulus are useful for assessing changes in the number of bound cross-bridges between experimental conditions. Shifts in the viscous modulus are useful for assessing changes in the work-producing and work-absorbing characteristics of the myocardium that arise from force-generating cross-bridges. Frequencies producing negative viscous moduli represent regions of work-producing muscle function. The “dip frequency” or frequency of the minimum viscous modulus describes force-generating events and cross-bridge recruitment rate (Campbell et al., 2004; Mulieri et al., 2002). Frequencies producing positive viscous moduli represent regions of work-absorbing muscle function. The “peak frequency” or frequency of the maximum viscous modulus describes cross-bridge distortion events and cross-bridge detachment rate (Campbell et al., 2004; Palmer et al., 2007, 2011). These characteristic regions of minima and maxima in the viscous modulus versus frequency relationship were used to assess effects of mavacamten on cross-bridge kinetics under maximal Ca^{2+} -activated conditions. Given that viscous moduli were only measured at discrete frequencies, polynomials were fitted to regions of minima viscous modulus (using 0.125- to 4-Hz data) and maxima viscous modulus (using 3- to 40-Hz data) using MATLAB to create fitted curves at 0.05-Hz resolution. From these interpolated curves, we extracted the frequency of minimum viscous modulus and frequency of maximum viscous modulus.

2.5 | Data and statistical analysis

The data and statistical analysis comply with the recommendations of the *British Journal of Pharmacology* on experimental design and analysis in pharmacology (Curtis et al., 2018). Experimental data were analysed in Statistical Analysis System (SAS; RRID: SCR_008567, version 9.4.3, SAS Institute, Cary, NC) using linear mixed effects models incorporating two main effects (drug treatment and sarcomere length) and their interaction for the stress-pCa fit parameters from Equation 1 and frequency parameters extracted from curve fits to the minima and maxima viscous moduli. These statistical analyses link data from the same hearts to optimize statistical power and can be considered as the two-way equivalent of a paired *t*-test (Haynes et al., 2014). Compound symmetry was assumed for the covariance structure, and post hoc analyses were performed using Tukey-Kramer corrections. *P* values less than 0.05 were considered significant.

2.6 | Nomenclature of targets and ligands

Key protein targets and ligands in this article are hyperlinked to corresponding entries in the IUPHAR/BPS Guide to PHARMACOLOGY <http://www.guidetopharmacology.org> (Harding et al., 2018) and are permanently archived in the Concise Guide to PHARMACOLOGY 2019/20 (Alexander et al., 2019).

3 | RESULTS

3.1 | Effects of mavacamten on Ca^{2+} -activated isometric contraction

Steady-state isometric stress (force normalized to cross-sectional area) was measured as activating $[\text{Ca}^{2+}]$ increased from pCa 8 (relaxed) to 4.5 (maximally activated) in myocardial strips isolated from donor hearts at 1.9- or 2.3- μm sarcomere length (Figure 2). For both sarcomere lengths, mavacamten decreased Ca^{2+} -activated force and reduced Ca^{2+} sensitivity of the force-pCa relationship. As sarcomere length increased, Ca^{2+} -activated force and Ca^{2+} sensitivity of the force-pCa relationship increased for control and mavacamten-treated myocardial strips. Therefore, the typical length-dependent activation response was maintained in the presence of mavacamten. Parameter values for 4-parameter Hill fits (Equation 1) to each stress-pCa relationship are summarized in Figure 3 (F_{act} and F_{pas}) and Figure 4 (pCa_{50} and n_{H}).

At 1.9- and 2.3- μm sarcomere length, 0.5- μM mavacamten significantly reduced Ca^{2+} -activated force by ~25%–30%, compared with control strips (Figure 3a). Ca^{2+} -activated force also significantly increased as sarcomere length increased. Similar findings occurred for passive force, with 0.5- μM mavacamten significantly reducing passive force at both sarcomere lengths (Figure 3b) and passive force significantly increasing as sarcomere length increased. These mavacamten-dependent decreases in passive force suggest that a portion of the passive force measured at pCa 8.0 arises from bound cross-bridges and that mavacamten stabilization of the myosin OFF state reduces this myosin-based contribution to passive force.

pCa_{50} values of the force-pCa relationship quantify the Ca^{2+} concentration required to produce half-maximal Ca^{2+} -activated force and describe the sensitivity of myocardial force to Ca^{2+} (Figure 4a). For both sarcomere lengths, 0.5- μM mavacamten significantly reduced the Ca^{2+} sensitivity of force by more than 0.1 pCa units compared with control (average $\Delta\text{pCa}_{50} = 0.17$ for 1.9- μm strips and $\Delta\text{pCa}_{50} = 0.12$ for 2.3- μm strips). The Ca^{2+} sensitivity of force also significantly increased as sarcomere length increased, exhibiting a length-dependent activation response for both control and mavacamten-treated strips. Hill coefficients (n_{H}) represent the degree of cooperativity (i.e. slope > 1) in the force-pCa relationship (Figure 4b), wherein mavacamten significantly increased n_{H} and sarcomere length did not significantly affect n_{H} .

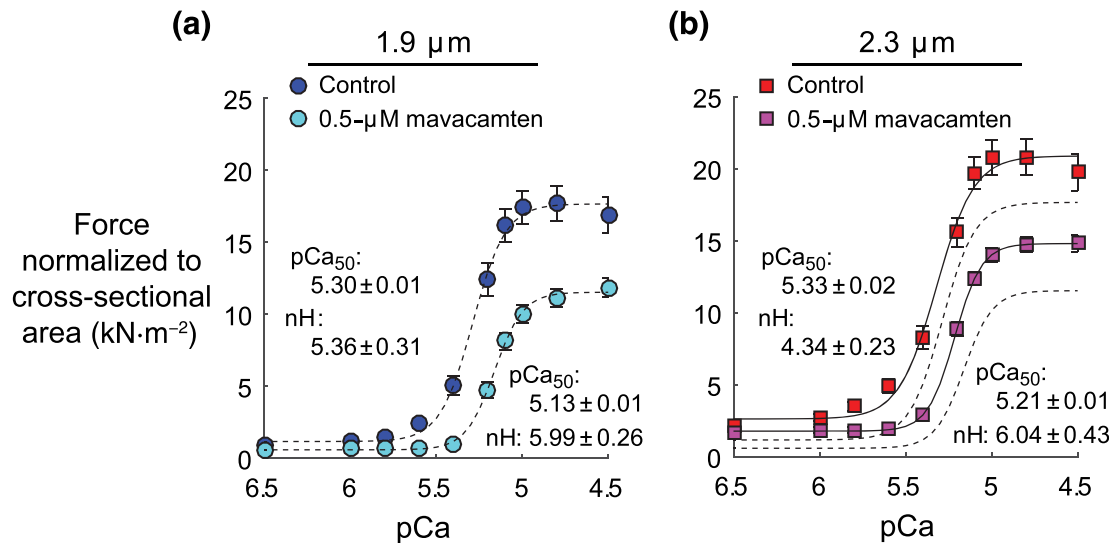


FIGURE 2 Effects of mavacamten on the isometric force–pCa relationship at 1.9- and 2.3- μm sarcomere length. (a and b) Steady-state force values (normalized to cross-sectional area of each myocardial strip) are plotted against pCa ($pCa = -\log_{10}[\text{Ca}^{2+}]$). Lines represent 4-parameter Hill fits to Equation 1. Dashed lines show fits at 1.9- μm sarcomere length, replotted in panel (b). Data were gathered from six hearts, with a total of 17 control strips and 18 mavacamten strips at 1.9- μm sarcomere length and 18 control strips and 17 mavacamten strips at 2.3- μm sarcomere length. Data are shown as mean \pm SEM, error bars within symbol if not visible

3.2 | Effects of mavacamten on myocardial viscoelasticity under maximal Ca^{2+} -activated conditions

Sinusoidal length–perturbation analysis was used to measure the myocardium's viscoelastic characteristics and the effects of mavacamten on cross-bridge recruitment and detachment rates at maximally activated conditions (pCa 4.5). For both sarcomere lengths, mavacamten reduced elastic moduli values across a wide range of frequencies (Figure 5a,b), indicating less cross-bridge binding in mavacamten-treated strips under maximally activated conditions. These decreases in cross-bridge binding also underlie the lower force values observed for mavacamten-treated strips (Figure 2), as changes in elastic moduli and isometric tension typically mirror each other.

Frequency shifts in the viscoelastic system response follow from changes in the enzymatic cross-bridge cycling kinetics under Ca^{2+} -activated conditions. These frequency shifts are most easily observed in the characteristic dips and peaks of the viscous modulus vs. frequency relationship (Figure 5c,d). Negative viscous moduli represent frequencies where the muscle produces work and positive viscous moduli represent frequencies where the muscle absorbs work. For both sarcomere lengths, mavacamten decreased the magnitude of negative viscous moduli, indicating less work production in mavacamten-treated strips than control strips. In addition, the frequencies where mavacamten-treated strips generated work were shifted towards lower frequencies. These shifts were quantified via the frequency of minimum viscous modulus for each strip (Figure 6a), indicating that cross-bridge recruitment rate slowed in mavacamten-treated strips (Campbell et al., 2004; Mulieri et al., 2002). Mavacamten also significantly increased the frequency

of maximum viscous modulus (Figure 6b), indicating that cross-bridge detachment rate increased in mavacamten-treated strips at physiological temperature.

4 | DISCUSSION

This study contributes new biophysical observations about how mavacamten alters contractility in human myocardium at body temperature. Early attempts to modulate sarcomere-level function in patients who have heart failure are showing promise (Heitner et al., 2019; Teerlink et al., 2016) and could be leveraged to improve patient care. Sarcomere length-dependent increases in the Ca^{2+} sensitivity of contraction are fundamental to the Frank–Starling response in healthy hearts. Accordingly, drugs that compromise length-dependent activation may be less effective therapies in patients (Gollapudi et al., 2017). Herein, we show that mavacamten preserves sarcomere length-dependent increases in the Ca^{2+} sensitivity of force, while reducing maximum levels of force production. Our data suggest that mavacamten may be a useful therapy for patients who have hypertrophic cardiomyopathy and a hypercontractile phenotype. It is less likely to help patients who have depressed contractile function. We also note that our data only quantify isometric force–length relationships and the rates of cross-bridge recruitment and detachment. Cardiac function ultimately depends on the power generated by myocytes during loaded shortening and future studies investigating the effect of mavacamten on the force–velocity relationship and/or pressure–volume loops in the whole heart would be useful (Campbell et al., 2020).

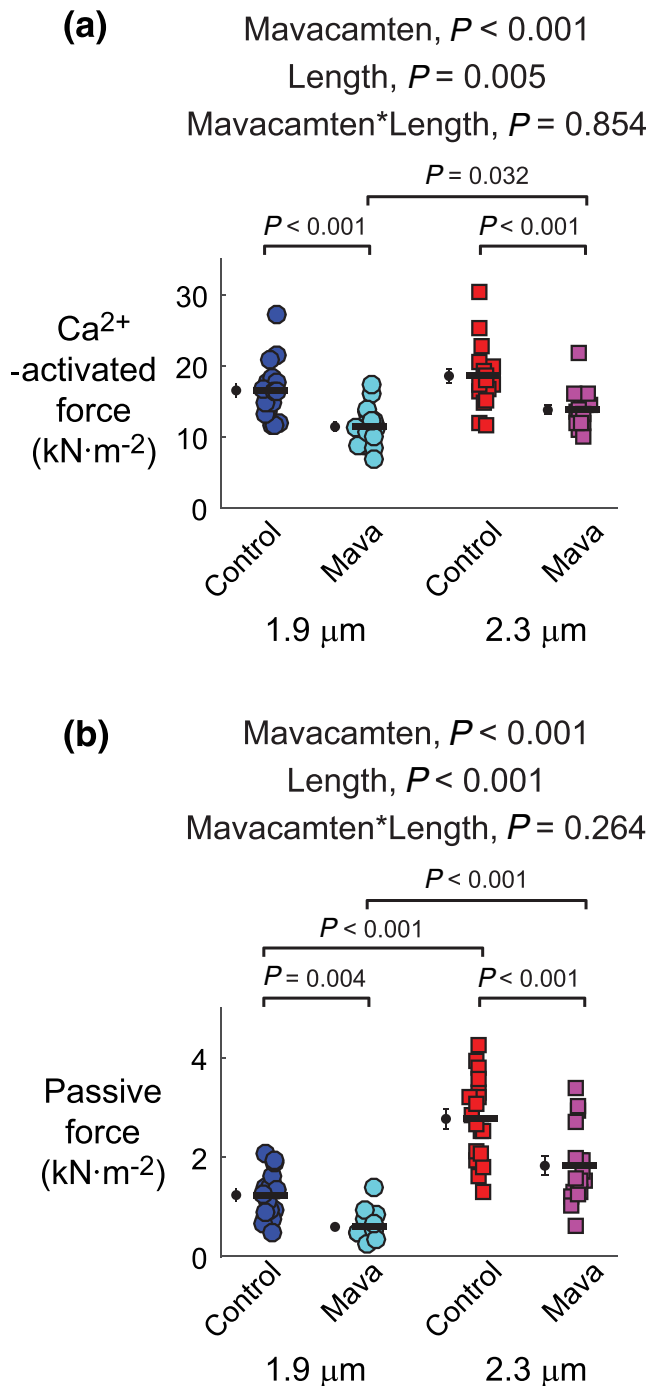


FIGURE 3 Effects of mavacamten on maximal Ca²⁺-activated force and passive force at 1.9- and 2.3- μ m sarcomere length. (a) Maximal and (b) passive force values from fits to Equation 1 are shown for each myocardial strip from each experimental group. Significant main effects and the associated interaction from linear mixed models analysis are listed above each panel for respective data therein. Jitter plots (coloured symbols) show measurements for each myocardial strip, with n listed in the legend of Figure 2. Black symbols show mean \pm SEM for each group plotted to the left of individual measurements

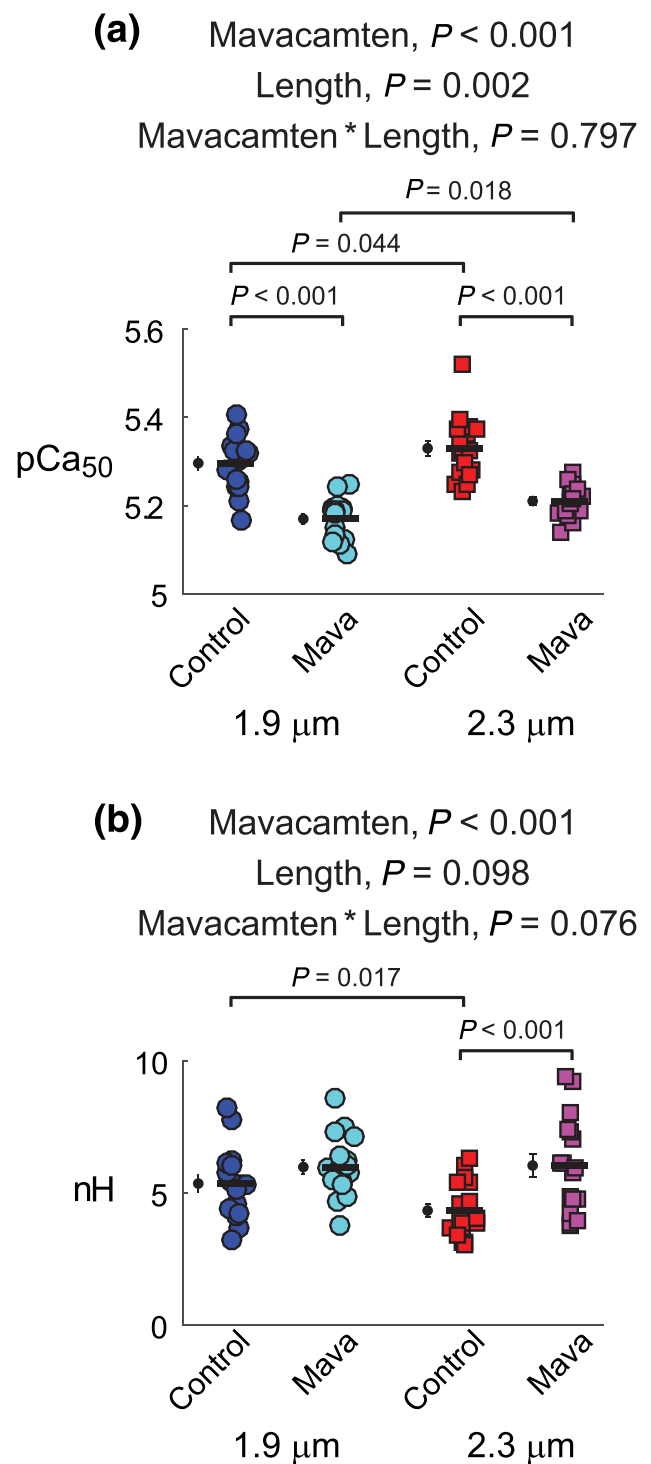


FIGURE 4 Effects of mavacamten on calcium activation of contraction at 1.9 and 2.3 μ m sarcomere length. (A) pCa₅₀ values and (B) n_H values from fits to Equation 1 are shown for each myocardial strip from each experimental group. Significant main effects and the associated interaction from linear mixed models analysis are listed above each panel for respective data therein. Jitter plots (coloured symbols) show measurements for each myocardial strip, with n listed in the legend of Figure 2. Black symbols show mean \pm SEM for each group plotted to the left of individual measurements

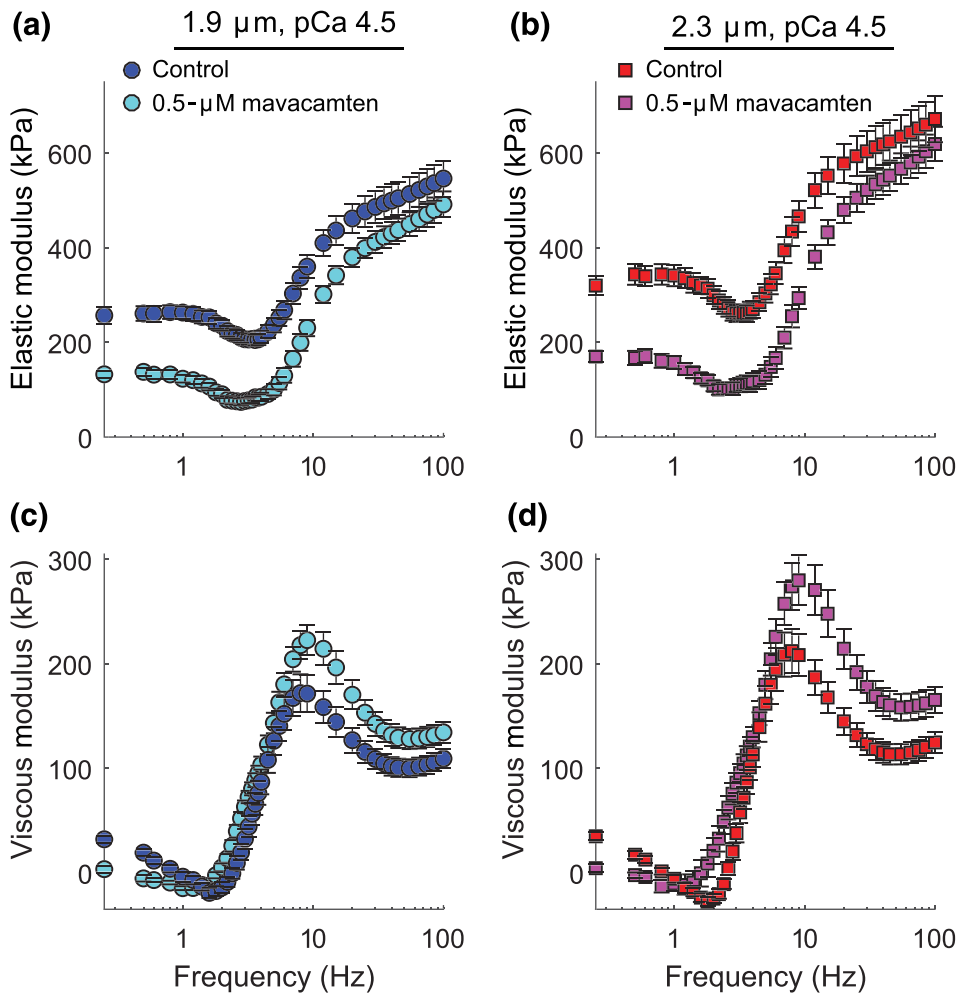


FIGURE 5 Effects of mavacamten on viscoelastic myocardial stiffness at pCa 4.5 for at 1.9- and 2.3- μm sarcomere length. (a and b) Elastic and (c and d) viscous moduli are plotted against frequency for maximal Ca^{2+} -activated conditions. Data are shown as mean \pm SEM, with n listed in the legend of Figure 2

The current data suggest that mavacamten will modulate both systolic and diastolic function. On the systolic side, hypertrophic cardiomyopathy has typically been viewed as a hypercontractile phenotype because of a “gain of function” mutation (Green et al., 2016; Moore et al., 2012). Mavacamten reduces Ca^{2+} sensitivity of contraction, which may reduce hypercontractility during systole and help to normalize contraction. Administering mavacamten early in life to transgenic mice that develop hypertrophic cardiomyopathy because of a R403Q mutation in myosin heavy chain reduced ventricular hypertrophy, cardiomyocyte disarray and myocardial fibrosis (Green et al., 2016). Thus, mavacamten may benefit hypertrophic cardiomyopathy patients with hypercontractility via reducing force and Ca^{2+} sensitivity during systole, potentially leading to beneficial remodelling of the heart.

Diastolic dysfunction is characterized by impaired relaxation and compromised ventricular filling and is present in at least 50% of patients who have heart failure (Aljaroudi et al., 2012; Lekavich et al., 2015; Mozaffarian et al., 2016). The data showing that mavacamten reduced passive tension at both sarcomere lengths (Figure 3b) and increased cross-bridge detachment rate under maximally activated conditions (Figure 6b) suggest that mavacamten may improve diastolic function (Sparrow et al., 2019; Sparrow et al., 2020;

Toefer et al., 2019, 2020). However, the measured decreases in passive tension with mavacamten treatment may not fully illustrate the effect of mavacamten on diastolic wall stress as the ventricle fills. One aspect of this involves greater cross-bridge contributions to diastolic function than we measured at pCa 8.0, because of estimated *in vivo* diastolic pCa levels of 6.0–5.6 that could augment thin-filament activation and diastolic wall stress (Bers, 2002). Another factor is that hypertrophic cardiomyopathy can increase intracellular $[\text{Ca}^{2+}]$ and $[\text{ADP}]$ above normal levels (Sequeira et al., 2015; Van Der Velden et al., 2018). These effects would normally enhance cross-bridge binding. Accordingly, mavacamten might have a greater effect in patients who have hypertrophic cardiomyopathy than was measured in this study that used myocardium from organ donors. Increases in myofilament Ca^{2+} sensitivity altered Ca^{2+} fluxes and poor metabolic homeostasis can lead to arrhythmias in some cases of hypertrophic cardiomyopathy (Baudenbacher et al., 2008; Schober et al., 2012). Thus, it is possible that mavacamten could play a cardioprotective role to resynchronize the timing of systolic and diastolic function.

Previously, we used mathematical models to test how mechanosensitive contributions of the myosin OFF–ON equilibrium influence length-dependent activation of contraction (Campbell

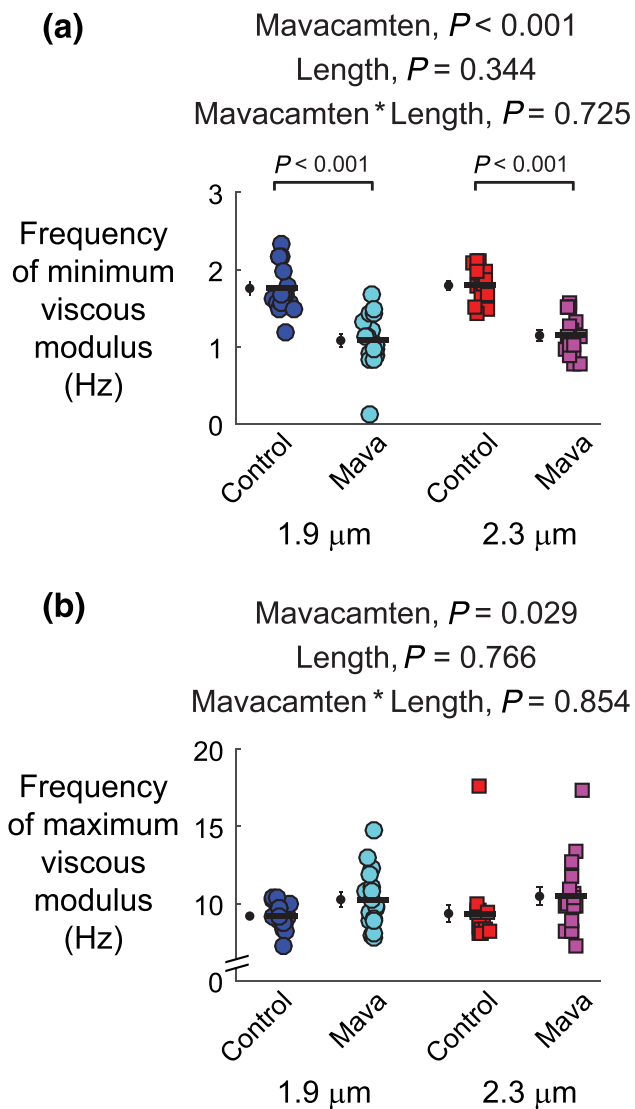


FIGURE 6 Effects of mavacamten on frequency-dependent shifts in the minimum and maximum viscous modulus at 1.9- and 2.3- μm sarcomere length. The (a) frequency producing the minimum viscous modulus and (b) frequency producing the minimum viscous modulus from polynomial fits to these associated regions of interest. Frequency shifts in the minimum and maximum viscous modulus describe relative changes in cross-bridge recruitment and detachment rates, respectively. Significant main effects and the associated interaction from linear mixed models analysis are listed above each panel for respective data therein. Jitter plots (coloured symbols) show measurements for each myocardial strip, with n listed in the legend of Figure 2. Black symbols show mean \pm SEM for each group plotted to the left of individual measurements

et al., 2018). These calculations showed that elevated passive and/or active force augmented cross-bridge recruitment and contributed to the dynamic regulation of contractility throughout a heartbeat (Figure 1). We wondered if sarcomere length-dependent increases in Ca^{2+} sensitivity would be amplified in mavacamten-treated strips. Our data do not show this response in a statistically significant manner

(Figure 4a), although the $p\text{Ca}_{50}$ change between 1.9 and 2.3 μm was threefold greater for mavacamten-treated strips (average $\Delta p\text{Ca}_{50} = 0.03$ for control vs. 0.09 for mavacamten strips). Our findings differ from a preliminary report using permeabilized myocardial strips from pigs, where mavacamten suppressed maximal force and blunted length-dependent increases in Ca^{2+} sensitivity (Henze et al., 2019). X-ray diffraction data also showed that a small population of cross-bridges remained sensitive to stretch, rather than completely abolished, in the presence of mavacamten (Henze et al., 2019).

Mavacamten stabilizes the OFF state (Figure 7) and shifts the OFF-ON equilibrium towards super-relaxed myosin (Anderson et al., 2018; Rohde et al., 2018; Toepfer et al., 2019, 2020). This reduces the number of heads that can bind to actin and generate force. Data supporting this mechanism include observations that mavacamten slows cross-bridge association, P_i release and actin-associated ADP release (Green et al., 2016; Kawas et al., 2017; Rohde et al., 2018). Mavacamten also slows the rate of force development in permeabilized myocardial strips from mice (Mamidi et al., 2018). Our viscoelastic stiffness measurements are also consistent with these findings (Figure 5) because mavacamten reduced the amount of work generated by the myocardium (Figure 5c,d) and the minimum frequency of the viscous modulus (Figure 6a). These data imply that mavacamten slows the weak-to-strong force bearing cross-bridge transition (Figure 7). It is also possible that mavacamten limits work production from the heart at the fastest heart rates, because the frequencies where myocardial strips generate negative viscous moduli typically reflect the physiological range of heart rates within a species. In summary, data from multiple studies consistently suggest that mavacamten stabilizes the OFF state, slows cross-bridge recruitment and slows P_i release to suppress myocardial force generation (Figure 7).

It is less clear how mavacamten affects cross-bridge detachment and myocardial relaxation. Multiple mechanisms may be involved. Biochemical studies show that mavacamten slows actin-independent ADP release (i.e. ADP dissociation rate in the absence of actin) (Kawas et al., 2017; Rohde et al., 2018). Other measurements show that mavacamten slows actin-myosin association rate when the reaction starts with unbound myosin in the ADP state (Kawas et al., 2017). While direct evidence that mavacamten slows ADP dissociation from strongly bound cross-bridges remains limited, mavacamten slows cross-bridge ATPase in mouse myofibrils where the rate limiting step is ADP release (Green et al., 2016). Our data show that mavacamten increases the frequency of peak viscous modulus (Figure 6b), indicating that mavacamten speeds cross-bridge detachment. Mavacamten also increases relaxation rate in human myofibrils (Scellini et al., 2020). Both observations could follow from mavacamten increasing the myosin-ATP association rate or the ATP affinity of myosin, though no data directly support this (Figure 7). Scellini et al. also show that mavacamten had no effect on relaxation rate in rabbit skeletal myofibrils, which suggests that the effects of mavacamten may vary with species and muscle type.

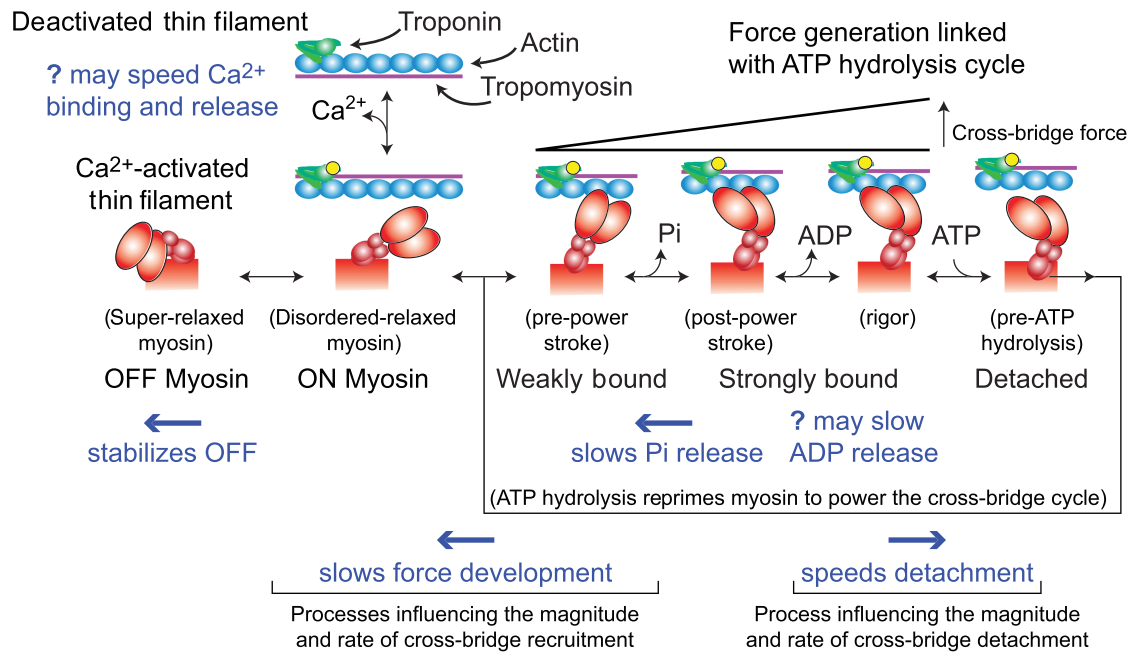


FIGURE 7 Schematic summarizing the effects of mavacamten on myocardial contractility at the myofilament level. Building from Figure 1, this schematic represents additional steps of the cross-bridge cycle associated with Pi and ADP release from myosin, ATP association and cross-bridge detachment, followed by ATP hydrolysis to reprime myosin for another force-generating event or relaxation. Blue text denotes known influences of mavacamten, which are further discussed in the text

Faster cross-bridge detachment could contribute to faster relaxation in mavacamten-treated cardiomyocytes (Sparrow et al., 2019; Sparrow et al., 2020; Toepfer et al., 2019, 2020). A component of this could involve thin filament dynamics (Figure 7) as Sparrow et al. used genetically encoded calcium indicators to show that mavacamten speeds the rates of Ca^{2+} binding and Ca^{2+} dissociation from troponin (Sparrow et al., 2019). These authors also showed that mavacamten decreased fluorescent intensity from these probes. This may follow from mavacamten decreasing the myosin ON population, which could attenuate myosin-based contributions to thin filament cooperativity. Changes in muscle length and force could also influence troponin dynamics, as X-ray diffraction measurements show that structural changes along thick filaments are concomitant with structural changes in thin filaments (Ait-Mou et al., 2016; Henze et al., 2019). Thus, mavacamten may affect Ca^{2+} binding to troponin in addition to modulating cross-bridge dynamics. These complex interactions reflect the dynamic coupling of the myofilaments.

The discovery of OFF–ON transitions within thick filaments reveals a new regulatory mechanism in cardiac muscle that could contribute to the Frank–Starling law. One particularly interesting aspect is the force-dependent recruitment of myosin to the ON state. This creates a force–feedback effect that enhances myosin-based generation during isometric and/or eccentric contractions (Ait-Mou et al., 2016; Brunello et al., 2020; Campbell, 2017; Fusi et al., 2017; Piazzesi et al., 2018; Reconditi et al., 2017; Zhang et al., 2017). Thus, any means of modulating length-dependent changes Ca^{2+} sensitivity may lead to significant functional effects on contraction and relaxation

dynamics in the heart. Prior to the discovery of force-dependent OFF–ON transitions, length-dependent changes in Ca^{2+} -sensitivity were thought to reflect changes in thin-filament function and/or the binding kinetics of individual myosin heads (Gordon et al., 2000). It is now clear that therapies targeting one of these mechanisms will have indirect effects on the other. Nevertheless, the current data provide new understanding about how mavacamten reduces contractility in human myocardium and bolster its potential as a therapy in patients who have hypertrophic cardiomyopathy and a hypercontractile phenotype (Ho et al., 2020). More generally, our findings suggest that the OFF–ON equilibrium of myosin may be an important therapeutic target in cardiac disease.

ACKNOWLEDGEMENTS

This work was supported by the American Heart Association (17SDG33370153 to B.C.W.T., 19TPA34860008 to B.C.W.T. and K.S.C. and GRNT25460003 to K.S.C.); the National Science Foundation (1656450 to B.C.W.T.); and the National Institutes of Health (R01HL149164 to B.C.W.T. and K.S.C. and TR001988, HL144664 and HL133358 to K.S.C.).

AUTHOR CONTRIBUTIONS

P.O.A., Y.B., M.W. and B.C.W.T. performed the research; P.O.A., M.G., K.S.C. and B.C.W.T. designed the research study; P.O.A., Y.B., M.W., M.G., K.S.C. and B.C.W.T. carried out the data and statistical analysis; P.O.A., M.G., K.S.C. and BCWT helped interpret data and potential clinical significance; P.O.A., K.S.C. and B.C.W.T. wrote the paper.

CONFLICT OF INTEREST

The authors declare no competing financial interests and have nothing to disclose.

DECLARATION OF TRANSPARENCY AND SCIENTIFIC RIGOUR

This Declaration acknowledges that this paper adheres to the principles for transparent reporting and scientific rigour of preclinical research as stated in the *BJP* guidelines for [Design & Analysis](#) and as recommended by funding agencies, publishers and other organizations engaged with supporting research.

ORCID

Kenneth S. Campbell  <https://orcid.org/0000-0001-5615-5958>

Bertrand C. W. Tanner  <https://orcid.org/0000-0003-1711-8526>

REFERENCES

- Ait-Mou, Y., Hsu, K., Farman, G. P., Kumar, M., Greaser, M. L., Irving, T. C., & de Tombe, P. P. (2016). Titin strain contributes to the Frank-Starling law of the heart by structural rearrangements of both thin- and thick-filament proteins. *Proceedings of the National Academy of Sciences of the United States of America*, *113*, 2306–2311. <https://doi.org/10.1073/pnas.1516732113>
- Alexander, S. P. H., Kelly, E., Mathie, A., Peters, J. A., Veale, E. L., Armstrong, J. F., ... Southan, C. (2019). The Concise Guide to PHARMACOLOGY 2019/20: Introduction and other protein targets. *British Journal of Pharmacology*, *176*, S1–S20.
- Aljaroudi, W., Alraies, M. C., Halley, C., Rodriguez, L., Grimm, R. A., Thomas, J. D., & Jaber, W. A. (2012). Impact of progression of diastolic dysfunction on mortality in patients with normal ejection fraction. *Circulation*, *125*, 782–788. <https://doi.org/10.1161/CIRCULATIONAHA.111.066423>
- Ambrosy, A. P., Fonarow, G. C., Butler, J., Chioncel, O., Greene, S. J., Vaduganathan, M., ... Gheorghiu, M. (2014). The global health and economic burden of hospitalizations for heart failure: Lessons learned from hospitalized heart failure registries. *Journal of the American College of Cardiology*, *63*, 1123–1133. <https://doi.org/10.1016/j.jacc.2013.11.053>
- Anderson, R. L., Trivedi, D. V., Sarkar, S. S., Henze, M., Ma, W., Gong, H., ... Spudich, J. A. (2018). Deciphering the super relaxed state of human beta-cardiac myosin and the mode of action of mavacamten from myosin molecules to muscle fibers. *Proceedings of the National Academy of Sciences of the United States of America*, *115*, E8143–E8152. <https://doi.org/10.1073/pnas.1809540115>
- Baudenbacher, F., Potter, J. D., Björn, C., Baudenbacher, F., Schober, T., Pinto, J. R., ... Knollmann, B. C. (2008). Myofilament Ca²⁺ sensitization causes susceptibility to cardiac arrhythmia in mice. *The Journal of Clinical Investigation*, *118*, 3893–3903.
- Bers, D. M. (2002). Cardiac excitation-contraction coupling. *Nature*, *415*, 198–205. <https://doi.org/10.1038/415198a>
- Blair, C. A., Haynes, P., Campbell, S. G., Chung, C., Mitov, M. I., Dennis, D., ... Campbell, K. S. (2016). A protocol for collecting human cardiac tissue for research. *The VAD Journal: The Journal of Mechanical Assisted Circulation and Heart Failure*, *2*(1), 12.
- Borlaug, B. A., & Paulus, W. J. (2011). Heart failure with preserved ejection fraction: Pathophysiology, diagnosis, and treatment. *European Heart Journal*, *32*, 670–679. <https://doi.org/10.1093/eurheartj/ehq426>
- Brandt, P. W., Lopez, E., Reuben, J. P., & Grundfest, H. (1967). The relationship between myofilament packing density and sarcomere length in frog striated muscle. *The Journal of Cell Biology*, *33*, 255–263. <https://doi.org/10.1083/jcb.33.2.255>
- Brunello, E., Fusi, L., Ghisleni, A., Park-Holohan, S. S. J., Ovejero, J. G., Narayanan, T., & Irving, M. (2020). Myosin filament-based regulation of the dynamics of contraction in heart muscle. *Proceedings of the National Academy of Sciences of the United States of America*, *117*, 8177–8186.
- Campbell, K. B., Chandra, M., Kirkpatrick, R. D., Slinker, B. K., & Hunter, W. C. (2004). Interpreting cardiac muscle force-length dynamics using a novel functional model. *American Journal of Physiology. Heart and Circulatory Physiology*, *286*, H1535–H1545.
- Campbell, K. S. (2017). Super-relaxation helps muscles work more efficiently. *The Journal of Physiology*, *595*, 1007–1008. <https://doi.org/10.1113/JP273629>
- Campbell, K. S., Chrisman, B. S., & Campbell, S. (2020). Multiscale modeling of cardiovascular function predicts that the end-systolic pressure volume relationship can be targeted via multiple therapeutic strategies. *Frontiers in Physiology*, *11*, 1043.
- Campbell, K. S., Janssen, P. M. L., & Campbell, S. G. (2018). Force-dependent recruitment from the myosin off state contributes to length-dependent activation. *Biophysical Journal*, *115*, 543–553. <https://doi.org/10.1016/j.bpj.2018.07.006>
- Cleland, J. G., Teerlink, J. R., Senior, R., Nifontov, E. M., Mc Murray, J. J., Lang, C. C., ... Malik, F. I. (2011). The effects of the cardiac myosin activator, omecamtiv mecarbil, on cardiac function in systolic heart failure: a double-blind, placebo-controlled, crossover, dose-ranging phase 2 trial. *Lancet*, *378*, 676–683. [https://doi.org/10.1016/S0140-6736\(11\)61126-4](https://doi.org/10.1016/S0140-6736(11)61126-4)
- Curtis, M. J., Alexander, S., Cirino, G., Docherty, J. R., George, G. H., Giembycz, M. A., ... Ahluwalia, A. (2018). Experimental design and analysis and their reporting II: updated and simplified guidance for authors and peer reviewers. *British Journal of Pharmacology*, *175*, 987–993. <https://doi.org/10.1111/bph.14153>
- Fusi, L., Brunello, E., Yan, Z., & Irving, M. (2016). Thick filament mechanosensing is a calcium-independent regulatory mechanism in skeletal muscle. *Nature Communications*, *7*, 13281.
- Fusi, L., Percario, V., Brunello, E., Caremani, M., Bianco, P., Powers, J. D., ... Piazzesi, G. (2017). Minimum number of myosin motors accounting for shortening velocity under zero load in skeletal muscle. *The Journal of Physiology*, *595*, 1127–1142. <https://doi.org/10.1113/JP273299>
- Godt, R. E., & Lindley, B. D. (1982). Influence of temperature upon contractile activation and isometric force production in mechanically skinned muscle fibers of the frog. *The Journal of General Physiology*, *80*, 279–297. <https://doi.org/10.1085/jgp.80.2.279>
- Gollapudi, S. K., Reda, S. M., & Chandra, M. (2017). Omecamtiv mecarbil abolishes length-mediated increase in guinea pig cardiac myofiber Ca²⁺ sensitivity. *Biophysical Journal*, *113*, 880–888. <https://doi.org/10.1016/j.bpj.2017.07.002>
- Gordon, A. M., Homsher, E., & Regnier, M. (2000). Regulation of contraction in striated muscle. *Physiological Reviews*, *80*, 853–924. <https://doi.org/10.1152/physrev.2000.80.2.853>
- Green, E. M., Wakimoto, H., Anderson, R. L., Evanchik, M. J., Gorham, J. M., Harrison, B. C., ... Seidman, C. E. (2016). A small-molecule inhibitor of sarcomere contractility suppresses hypertrophic cardiomyopathy in mice. *Science* (80-), *351*, 617–621. <https://doi.org/10.1126/science.aad3456>
- Grillo, M. P., Erve, J. C. L., Dick, R., Driscoll, J. P., Haste, N., Markova, S., ... Evanchik, M. (2018). In vitro and in vivo pharmacokinetic characterization of mavacamten, a first-in-class small molecule allosteric modulator of beta cardiac myosin. *Xenobiotica*, *49*(6), 718–733.
- Harding, S. D., Sharman, J. L., Faccenda, E., Southan, C., Pawson, A. J., Ireland, S., ... NC-IUPHAR. (2018). The IUPHAR/BPS guide to PHARMACOLOGY in 2018: Updates and expansion to encompass the new guide to IMMUNOPHARMACOLOGY. *Nucleic Acids Research*, *46*, D1091–D1106. <https://doi.org/10.1093/nar/gkx1121>
- Haynes, P., Nava, K. E., Lawson, B. A., Chung, C. S., Mitov, M. I., Campbell, S. G., ... Campbell, K. S. (2014). Transmural heterogeneity of

- cellular level power output is reduced in human heart failure. *Journal of Molecular and Cellular Cardiology*, 72, 1–8. <https://doi.org/10.1016/j.yjmcc.2014.02.008>
- Heitner, S. B., Jacoby, D., Lester, S. J., Owens, A., Wang, A., Zhang, D., ... Sehnert, A. J. (2019). Mavacamten treatment for obstructive hypertrophic cardiomyopathy a clinical trial. *Annals of Internal Medicine*, 170, 741–748. <https://doi.org/10.7326/M18-3016>
- Henze, M., Ma, W., Wong, F., Gong, H., Anderson, R. L., del Rio, C., & Irving, T. C. (2019). Length dependent activation in porcine cardiac myofilaments is modulated by mavacamten. *Circulation Research*, 125 (Suppl_1), A905–A905.
- Ho, C. Y., Carlsen, C., Thune, J. J., Havndrup, O., Bundgaard, H., Farrohi, F., ... Køber, L. (2009). Echocardiographic strain imaging to assess early and late consequences of sarcomere mutations in hypertrophic cardiomyopathy. *Circulation. Cardiovascular Genetics*, 2, 314–321. <https://doi.org/10.1161/CIRCGENETICS.109.862128>
- Ho, C. Y., Mealiffe, M. E., Bach, R. G., Bhattacharya, M., Choudhury, L., Edelberg, J. M., ... Heitner, S. B. (2020). Evaluation of mavacamten in symptomatic patients with nonobstructive hypertrophic cardiomyopathy. *Journal of the American College of Cardiology*, 75, 2649–2660. <https://doi.org/10.1016/j.jacc.2020.03.064>
- Hooijman, P., Stewart, M. A., & Cooke, R. (2011). A new state of cardiac myosin with very slow ATP turnover: A potential cardioprotective mechanism in the heart. *Biophysical Journal*, 100, 1969–1976. <https://doi.org/10.1016/j.bpj.2011.02.061>
- Huxley, H., & Hanson, J. (1954). Changes in the cross-striations of muscle during contraction and stretch and their structural interpretation. *Nature*, 173, 973–976. <https://doi.org/10.1038/173973a0>
- Kampourakis, T., Sun, Y.-B., & Irving, M. (2016). Myosin light chain phosphorylation enhances contraction of heart muscle via structural changes in both thick and thin filaments. *Proceedings of the National Academy of Sciences of the United States of America*, 113, E3039–E3047. <https://doi.org/10.1073/pnas.1602776113>
- Kawai, M., & Brandt, P. (1980). Sinusoidal analysis: A high resolution method for correlating biochemical reactions with physiological processes in activated skeletal muscles of rabbit, frog and crayfish. *Journal of Muscle Research and Cell Motility*, 1, 279–303. <https://doi.org/10.1007/BF00711932>
- Kawas, R. F. F., Anderson, R. L., Ingle, S. R. B., Song, Y., Sran, A. S., & Rodriguez, H. M. (2017). A small-molecule modulator of cardiac myosin acts on multiple stages of the myosin chemomechanical cycle. *The Journal of Biological Chemistry*, 292, 16571–16577. <https://doi.org/10.1074/jbc.M117.776815>
- Klein, M. D., Lane, F. J., & Gorlin, R. (1965). Effect of left ventricular size and shape upon the hemodynamics of subaortic stenosis. *The American Journal of Cardiology*, 15, 773–781. [https://doi.org/10.1016/0002-9149\(65\)90379-6](https://doi.org/10.1016/0002-9149(65)90379-6)
- Lekavich, C. L., Barksdale, D. J., Neelon, V., & Wu, J. R. (2015). Heart failure preserved ejection fraction (HFpEF): An integrated and strategic review. *Heart Failure Reviews*, 20, 643–653. <https://doi.org/10.1007/s10741-015-9506-7>
- Linari, M., Brunello, E., Reconditi, M., Fusi, L., Caremani, M., Narayanan, T., ... Irving, M. (2015). Force generation by skeletal muscle is controlled by mechanosensing in myosin filaments. *Nature*, 528, 276–279. <https://doi.org/10.1038/nature15727>
- Liu, C., Kawana, M., Song, D., Ruppel, K. M., & Spudich, J. A. (2018). Controlling load-dependent kinetics of β -cardiac myosin at the single-molecule level. *Nature Structural & Molecular Biology*, 25, 505–514. <https://doi.org/10.1038/s41594-018-0069-x>
- Lymn, R. W., & Taylor, E. W. (1971). Mechanism of adenosine triphosphate hydrolysis by actomyosin. *Biochemistry*, 10, 4617–4624. <https://doi.org/10.1021/bi00801a004>
- Malik, F. I., Hartman, J. J., Elias, K. A., Morgan, B. P., Rodriguez, H., Brejc, K., ... Morgans, D. J. (2011). Cardiac myosin activation: A potential therapeutic approach for systolic heart failure. *Science* (80-), 331, 1439–1443. <https://doi.org/10.1126/science.1200113>
- Mamidi, R., Li, J., Doh, C. Y., Verma, S., & Stelzer, J. E. (2018). Impact of the myosin modulator mavacamten on force generation and cross-bridge behavior in a murine model of hypercontractility. *Journal of the American Heart Association*, 7, e009627.
- Maron, B. J., Gardin, J. M., Flack, J. M., Gidding, S. S., Kurosaki, T. T., & Bild, D. E. (1995). Prevalence of hypertrophic cardiomyopathy in a general population of young adults: Echocardiographic analysis of 4111 subjects in the CARDIA study. *Circulation*, 92, 785–789. <https://doi.org/10.1161/01.cir.92.4.785>
- McNamara, J. W., Li, A., Lal, S., Bos, J. M., Harris, S. P., Van Der Velden, J., ... Dos Remedios, C. G. (2017). MYBPC3 mutations are associated with a reduced super-relaxed state in patients with hypertrophic cardiomyopathy. *PLoS ONE*, 12, e0180064.
- McNamara, J. W., Li, A., Remedios, C. G. D., & Cooke, R. (2015). The role of super-relaxed myosin in skeletal and cardiac muscle. *Biophysical Reviews*, 7, 5–14. <https://doi.org/10.1007/s12551-014-0151-5>
- Michels, M., Soliman, O. I. I., Kofflard, M. J., Hoedemaekers, Y. M., Dooijes, D., Majoor-Krakauer, D., & ten Cate, F. J. (2009). Diastolic abnormalities as the first feature of hypertrophic cardiomyopathy in dutch myosin-binding protein C founder mutations. *JACC: Cardiovascular Imaging*, 2, 58–64. <https://doi.org/10.1016/j.jcmg.2008.08.003>
- Moore, J. R., Leinwand, L., & Warshaw, D. M. (2012). Understanding cardiomyopathy phenotypes based on the functional impact of mutations in the myosin motor. *Circulation Research*, 111, 375–385. <https://doi.org/10.1161/CIRCRESAHA.110.223842>
- Mozaffarian, D., Benjamin, E. J., Go, A. S., Arnett, D. K., Blaha, M. J., Cushman, M., ... Howard, V. J. (2016). Heart disease and stroke statistics-2016 update a report from the American Heart Association. *Circulation*, 133(4), e38–e48.
- Mulieri, L. A., Barnes, W. D., Leavett, B. J., Ittleman, F., LeWinter, M. M., Alpert, N. R., & Maughan, D. W. (2002). Alterations of myocardial dynamic stiffness implicating abnormal crossbridge function in human mitral regurgitation heart failure. *Circulation Research*, 90, 66–72. <https://doi.org/10.1161/hh0102.103221>
- Palmer, B. M., Suzuki, T., Wang, Y., Barnes, W. D., Miller, M. S., & Maughan, D. W. (2007). Two-state model of acto-myosin attachment-detachment predicts C-process of sinusoidal analysis. *Biophysical Journal*, 93, 760–769. <https://doi.org/10.1529/biophysj.106.101626>
- Palmer, B. M., Wang, Y., & Miller, M. S. (2011). Distribution of myosin attachment times predicted from viscoelastic mechanics of striated muscle. *Journal of Biomedicine & Biotechnology*, 2011, 592343.
- Piazzesi, G., Caremani, M., Linari, M., Reconditi, M., & Lombardi, V. (2018). Thick filament mechano-sensing in skeletal and cardiac muscles: A common mechanism able to adapt the energetic cost of the contraction to the task. *Frontiers in Physiology*, 9, 736.
- Reconditi, M., Caremani, M., Pinzauti, F., Powers, J. D., Narayanan, T., Stienen, G. J. M., ... Piazzesi, G. (2017). Myosin filament activation in the heart is tuned to the mechanical task. *Proceedings of the National Academy of Sciences of the United States of America*, 114, 3240–3245. <https://doi.org/10.1073/pnas.1619484114>
- Rohde, J. A., Roopnarine, O., Thomas, D. D., Muretta, J., & Hall, J. (2018). Mavacamten stabilizes an autoinhibited state of two-headed cardiac myosin. *Proceedings of the National Academy of Sciences of the United States of America*, 115, E7486–E7494. <https://doi.org/10.1073/pnas.1720342115>
- Scellini, B., Piroddi, N., Dente, M., Ferrantini, C., Coppini, R., Poggesi, C., & Tesi, C. (2020). Impact of mavacamten on force generation in single myofibrils from rabbit psoas and human cardiac muscle. *Biophysical Journal*, 118, 7a.
- Schober, T., Huke, S., Venkataraman, R., Gryshchenko, O., Kryshal, D., Hwang, H. S., ... Knollmann, B. C. (2012). Myofilament Ca sensitization increases cytosolic Ca binding affinity, alters intracellular Ca

- homeostasis, and causes pause-dependent Ca-triggered arrhythmia. *Circulation Research*, 111, 170–179. <https://doi.org/10.1161/CIRCRESAHA.112.270041>
- Semsarian, C., Ingles, J., Maron, M. S., & Maron, B. J. (2015). New perspectives on the prevalence of hypertrophic cardiomyopathy. *Journal of the American College of Cardiology*, 65, 1249–1254. <https://doi.org/10.1016/j.jacc.2015.01.019>
- Sequeira, V., Najafi, A., McConnell, M., Fowler, E. D., Bollen, I. A. E., Wüst, R. C. I., ... Tardiff, J. (2015). Synergistic role of ADP and Ca²⁺ in diastolic myocardial stiffness. *The Journal of Physiology*, 593, 3899–3916. <https://doi.org/10.1113/JP270354>
- Sparrow, A. J., Sievert, K., Patel, S., Chang, Y. F., Broyles, C. N., Brook, F. A., ... Daniels, M. J. (2019). Measurement of myofilament-localized calcium dynamics in adult cardiomyocytes and the effect of hypertrophic cardiomyopathy mutations. *Circulation Research*, 124, 1228–1239. <https://doi.org/10.1161/CIRCRESAHA.118.314600>
- Sparrow, A. J., Watkins, H., Daniels, M. J., Redwood, C., & Robinson, P. (2020). Mavacamten rescues increased myofilament calcium sensitivity and dysregulation of Ca²⁺ flux caused by thin filament hypertrophic cardiomyopathy mutations. *American Journal of Physiology. Heart and Circulatory Physiology*, 318, H715–H722. <https://doi.org/10.1152/ajpheart.00023.2020>
- Spudich, J. A. (2015). The myosin mesa and a possible unifying hypothesis for the molecular basis of human hypertrophic cardiomyopathy. *Biochemical Society Transactions*, 43, 64–72. <https://doi.org/10.1042/BST20140324>
- Stern, J. A., Markova, S., Ueda, Y., Kim, J. B., Pascoe, P. J., Evanchik, M. J., ... Harris, S. P. (2016). A small molecule inhibitor of sarcomere contractility acutely relieves left ventricular outflow tract obstruction in feline hypertrophic cardiomyopathy. *PLoS ONE*, 11, e0168407. <https://doi.org/10.1371/journal.pone.0168407>
- Stewart, S., Mason, D. T., & Braunwald, E. (1968). Impaired rate of left ventricular filling in idiopathic hypertrophic subaortic stenosis and valvular aortic stenosis. *Circulation*, 37, 8–14. <https://doi.org/10.1161/01.cir.37.1.8>
- Teerlink, J. R., Felker, G. M., McMurray, J. J. V., Solomon, S. D., Adams, K. F., Cleland, J. G., ... Mitrovic, V. (2016). Chronic oral study of myosin activation to increase contractility in heart failure (COSMIC-HF): a phase 2, pharmacokinetic, randomised, placebo-controlled trial. *Lancet*, 388, 2895–2903. [https://doi.org/10.1016/S0140-6736\(16\)32049-9](https://doi.org/10.1016/S0140-6736(16)32049-9)
- Toepfer, C. N., Caorsi, V., Kampourakis, T., Sikkil, M. B., West, T. G., Leung, M.-C., ... Sellers, J. R. (2013). Myosin regulatory light chain (RLC) phosphorylation change as a modulator of cardiac muscle contraction in disease. *The Journal of Biological Chemistry*, 288, 13446–13454. <https://doi.org/10.1074/jbc.M113.455444>
- Toepfer, C. N., Garfinkel, A. C., Venturini, G., Wakimoto, H., Repetti, G., Alamo, L., ... Seidman, C. E. (2020). Myosin sequestration regulates sarcomere function, cardiomyocyte energetics, and metabolism, informing the pathogenesis of hypertrophic cardiomyopathy. *Circulation*, 141, 828–842. <https://doi.org/10.1161/CIRCULATIONAHA.119.042339>
- Toepfer, C. N., Wakimoto, H., Garfinkel, A. C., McDonough, B., Liao, D., Jiang, J., ... Seidman, C. E. (2019). Hypertrophic cardiomyopathy mutations in MYBPC3 dysregulate myosin. *Science Translational Medicine*, 11, eaat1199. <https://doi.org/10.1126/scitranslmed.aat1199>
- Toepfer, C. N., West, T. G., & Ferenczi, M. A. (2016). Revisiting Frank–Starling: Regulatory light chain phosphorylation alters the rate of force redevelopment (ktr) in a length-dependent fashion. *The Journal of Physiology*, 594, 5237–5254. <https://doi.org/10.1113/JP272441>
- Tuohy, C. V., Kaul, S., Song, H. K., Nazer, B., & Heitner, S. B. (2020). Hypertrophic cardiomyopathy: The future of treatment. *European Journal of Heart Failure*, 22, 228–240. <https://doi.org/10.1002/ejhf.1715>
- Van Der Velden, J., Tocchetti, C. G., Varricchi, G., Bianco, A., Sequeira, V., Hilfiker-Kleiner, D., ... Thum, T. (2018). Metabolic changes in hypertrophic cardiomyopathies: Scientific update from the working group of myocardial function of the European Society of Cardiology. *Cardiovascular Research*, 114, 1273–1280.
- Wilson, W. S., Criley, J. M., & Ross, R. S. (1967). Dynamics of left ventricular emptying in hypertrophic subaortic stenosis. A cineangiographic and hemodynamic study. *American Heart Journal*, 73, 4–16. [https://doi.org/10.1016/0002-8703\(67\)90303-1](https://doi.org/10.1016/0002-8703(67)90303-1)
- Zhang, X., Kampourakis, T., Yan, Z., Sevrieva, I., Irving, M., & Sun, Y.-B. (2017). Distinct contributions of the thin and thick filaments to length-dependent activation in heart muscle. *eLife*, 6, e24081.

How to cite this article: Awinda PO, Bishaw Y, Watanabe M, Guglin MA, Campbell KS, Tanner BCW. Effects of mavacamten on Ca²⁺ sensitivity of contraction as sarcomere length varied in human myocardium. *Br J Pharmacol*. 2020; 177:5609–5621. <https://doi.org/10.1111/bph.15271>